ME 502 PROJECT 1

RADIATOR OF AUTOMOBILES

February 5, 2023

Net ID: jiongc2
Name: Jiong Chen
University of Illinois at Urbana-Champaign
Department of Mechanical Engineering

Contents

ABSTRACT

Radiators are a crucial part in automobiles. In this project, a engine-cooling radiator of one-slab one-pass with horizontal flat tubes and louver-fins is simulated. The simulation evaluates the thermal performance and the hydraulic performance of the radiator with the finite volume concept. The simulation is accomplished by Python and package CoolProp is used for retrieving the thermal properties. For thermal performance, $\epsilon - NTU$ method is used for calculation of heat transfer rate; empirical correlations are adopted for heat transfer coefficient, j-Colburn factor and friction factor. The simulation considered the impact of element numbers through the tube to the performance evaluation. Larger mesh size can lead to more accurate result; however, it can also increase computation load. Keep increasing mesh size will result in small improvement of accuracy but more computation work. The best mesh size is determined.

INTRODUCTION

For a traditional automobile, with the engine is designed, a radiator which can maintain the engine working at safe temperature is critical. If the radiator design cannot dissipate the heat generated during the operation of the engine, the temperature of the engine will increase to a dangerous range, which will lead to the performance drop of the engine and also decreasing life time of the engine. And in order to limit the cost of the automobile, the radiator should not be "overdesigned". Thus, optimize the design of radiator is important in automobile design. Besides, the radiator can control the cabin temperature by interacting with heater in the car.

The main parts of a radiator are radiator core, thermostat valve, water pump and engine driven fan. As Figure. 1 shows, the coolant will loop from the bottom of the radiator and leaves the radiator at the top tank; if the temperature of the engine is high, the thermostat valve will be opened and the coolant can enter the engine; after the coolant loops through the engine, it passes the water pump and re-enters the radiator core. The hot coolant can be cooled by the cold air flow through the radiator.

In common conditions, the engine coolants are usually water-ethylene glycol (EG), and this project, the coolant used for the radiator is water-ethylene glycol (EG) solution with a mass fraction of 50% for ethylene. The geometrical information of the radiator is included in Table 1 and Table 2. And the corresponded illustration of each parameter are indicated on Figure 2. Figure 3 shows the schematic of the radiator. For simplify the simulation, assumptions are

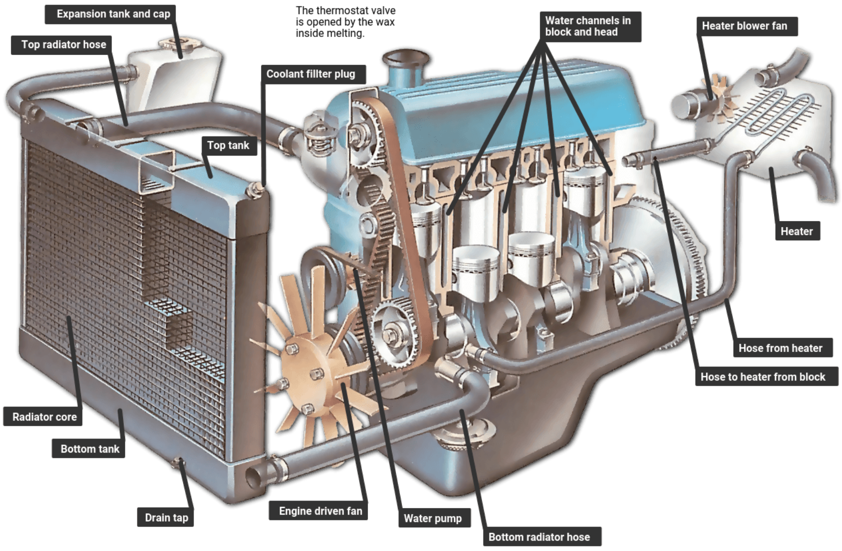

Figure 1: Radiator Design

Tube Geometry	Size
N_{slab}: number pf slabs (rows), [-]	1
N_{pass}: number of passes in one slab, [-]	1
$L_{tube,pass}$: tube length in one pass, [mm]	700
$N_{tube,pass}$: number of tubes in one pass, [-]	40
$t_{wall}*$: wall thickness, [mm]	0.35
t_{tube}: tube thickness, [mm]	3
D_{tube}: tube depth, [mm]	35
N_{port}: number of ports in one tube, [-]	3
Ra_{tube}: roughness of tube inner surface, [m]	10^{-6}

$^*t_{wall}$: assume all the outer walls and inner walls have the same thickness

Table 1: Dimensions of the tubes of the radiator

made: uniform mass flow rate of water-EG in each tube and uniform mass flow rate of air for each element. Along the tube flow direction, tube is divided into small segments. Each segment's input is the output of the former segment, and the output will be the next segment's input. Detailed equations are presented in Methods part. The operating conditions of the radiator is listed in Table 3.

METHODS

For Methods, it consists of two parts: thermal and hydraulic.
For thermal calculation, air is assumed to be ideal gas, no condensation included. The tube

Fin Geometry	Size
θ_{louver}: louver angle, [deg]	18
P_{louver}: louver pitch , [mm]	1.2
L_{louver}: louver length, [mm]	9
$N_{louverbank}$: number of louvers sets per fin, [-]	2
h_{fin}: fin height, [mm]	10
t_{fin}: fin thickness, [mm]	0.1
P_{fin}: fin pitch, [mm]	1.4 (18 FPI*)
D_{fin}: Depth of fin, [mm]	35

*FPI: fin per inch

Table 2: Dimensions of the fins of the radiator

Parameter	Value
T_{ri}: refrigerant inlet temperature, [C]	75
P_{ri}: refrigerant inlet pressure , [kPa]	150
$\dot{V}_r$: refrigerant volumetric flow rate, [L/min]	40
T_{ai}: air inlet temperature, [C]	25
P_{ai}: air inlet pressure, [kPa]	99.5
$\dot{m}_a$: air mass flow rate, [kg/h]	5000

Table 3: Dimensions of the fins of the radiator

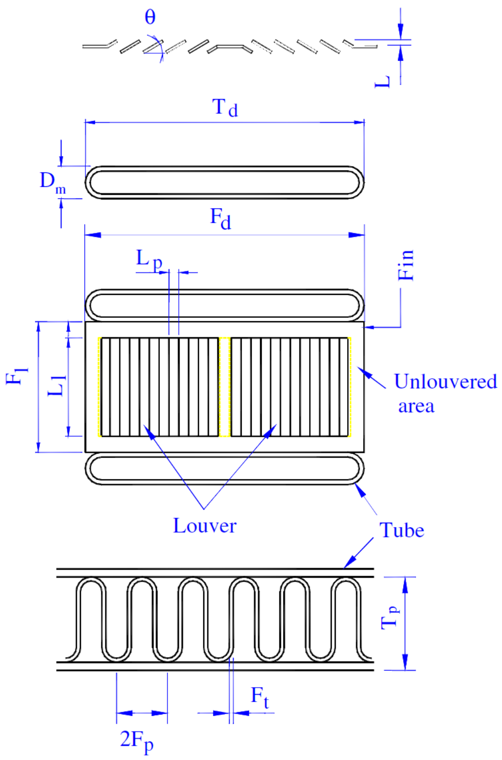

Figure 2: Definition of various geometric parameters for corrugated louver fin [1]

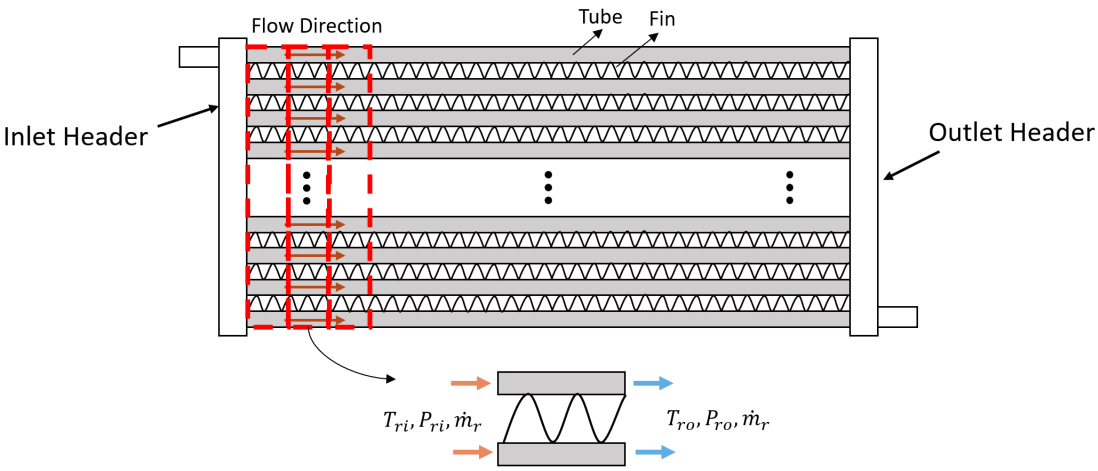

Figure 3: Radiator Schematic

wall thermal resistance is neglected. And the thermal conductivity of metal is assumed to be constant. heat transfer coefficient (htc) for air side and coolant side is calculated according to Chang and Wang's correlation [2], and Nusselt number for laminar flow and Gnielinski correlation for turbulent flow. Since the air inlet flow temperature and pressure are the same for each element, the air side htc only needs to be calculate once with following step:

$$htc_{air} = \rho_{air} \times Vel_{air} \times Cp_{air} \times St \tag{1}$$

$$St = j \times Pr_{air}^{-2/3} \tag{2}$$

$$Vel_{air} = \frac{\dot{m}_a}{\rho_{air} A_{air,free}} \tag{3}$$

$$A_{air,free} = A_{front} - A_{ft,cross} \tag{4}$$

$$A_{ft,cross} = (N_{tube,pass} N_{pass} t_{tube} L_{tube,pass}) - (N_{tube,pass} N_{pass} - 1) L_{tube,pass} P_{fin} h_{fin} t_{fin} \tag{5}$$

The j, j-Colburn factor in equation (2) can be calculated with Chang and Wang's correlation[?], which depends on the geometry of the fin and tube:

$$\begin{aligned} j = Re_{Lp}^{-0.49} \left(\frac{\theta_{louver}}{90}\right)^{0.27} \left(\frac{P_{fin}}{P_{louver}}\right)^{-0.14} \left(\frac{h_{fin}}{P_{louver}}\right)^{-0.29} \left(\frac{D_{tube}}{P_{louver}}\right)^{-0.23} \\ \left(\frac{L_{louver}}{P_{louver}}\right)^{0.68} \left(\frac{P_{tube}}{P_{louver}}\right)^{-0.28} \left(\frac{t_{fin}}{P_{louver}}\right)^{-0.05} \end{aligned} \tag{6}$$

Cross Section	$\frac{b}{a}$	$Nu_D = \frac{HTC \cdot D_h}{k}$ (Uniform q_s'')	(Uniform T_s)
	—	4.36	3.66
a b	1.0	3.61	2.98
a b	1.43	3.73	3.08
a b	2.0	4.12	3.39
a b	3.0	4.79	3.96
a b	4.0	5.33	4.44
a b	8.0	6.49	5.60
	∞	8.23	7.54
Heated / Insulated	∞	5.39	4.86
	—	3.11	2.49

Table 4: Nusselt number for laminar internal flow

$$Re_{Lp} = \frac{\rho_{air} Vel_{air} P_{louver}}{\mu_{air}} \tag{7}$$

For refrigerant side htc, for the fully developed internal laminar flow, Nu is calculated according to Table 4 from Heat Transfer Textbook. Due to complex wall condition, Nu is taken as the average number of uniform heat flux case and uniform wall temperature case. Data interpolation is used to calculate the condition that $\frac{b}{a}$ is not the case in the table. The interpolation method used in the simulation is Python package interpolate with method UnivariateSpline. For the flow $Re_D > 2300$, which is turbulent, Nu can be calculated with Gnielinski correlation [3]:

$$f = (0.79 \ln Re_D - 1.64)^{-2} \tag{8}$$

$$Nu_D = \frac{\frac{f}{8}(Re_D - 1000)Pr}{1 + 12.7\left(\frac{f}{8}\right)^{1/2}(Pr^{(\frac{2}{3})} - 1)} \tag{9}$$

$$htc_{ref} = \frac{Nu_D k_r ef}{D_{h,port}} \tag{10}$$

$$D_{h,port} = \frac{4A_{port}}{P_{port}} \tag{11}$$

$$A_{port} = (N_{port}-2)(H_{port}W_{port}) + 2((W_{port} - \frac{H_{port}}{2})H_{port} + \pi\frac{H_{port}^2}{4}) \tag{12}$$

$$P_{port} = 2(H_{port}+W_{port})(N_{port}-2) + 2(H_{port} + 2(W_{port} - \frac{H_port}{2}) \tag{13}$$

$$H_{port} = t_{tube} - 2t_{wall} \tag{14}$$

$$W_{port} = (D_{tube} - (N_{port}+1)\,t_{wall}/N_{port} \tag{15}$$

With htc_{air} and htc_{ref}, using $\epsilon - NTU$ method:

$$Q = \sigma C_{min}(T_{ri} - T_{ai}) \tag{16}$$

$$\sigma = 1 - \exp(\frac{1}{C_{ratio}}NTU^{0.22}(\exp(-C_{ratio}NTU^{0.78}) - 1)) \tag{17}$$

$$NTU = \frac{UA}{C_{min}} \tag{18}$$

$$UA = \frac{1}{R_{air} + \frac{1}{htc_{ref}A_{ref,elem}}} \tag{19}$$

$$R_{air} = \frac{1}{htc_{air}A_{air,elem}\eta} \tag{20}$$

$$T_{ro} = T_{ri} - Q/C_{ref} \tag{21}$$

$$T_{ao} = T_{ai} + Q/C_{air} \tag{22}$$

in equation (20), η is the overall fin efficiency. $A_{air,elem}$ and $A_{ref,elem}$ are air side heat transfer area and refrigerant side heat transfer area for each element respectively. Thus, the heat transfer rate of each element is calculated, and the outlet air temperature, outlet water-EG temperature can be obtained by equation (21) and (22).

For hydraulic performance, Churchill's [4] correlation is adopted for water-EG and Chang and Wang's [5] Correlation is adopted for air side. The pressure drop of water-EG consists of static pressure, hydrostatic pressure and dynamic pressure. Consider that all the tubes are horizontal, the hydrostatic pressure can be neglected; for one segment, the velocity of coolant change is negligible so that dynamic pressure can be neglected. The main contribution to pressure drop is static pressure which caused by friction. Pressure drop in tube can be calculated as following:

$$DP_{ref} = DP_{ref,static} = \frac{\partial p}{\partial z}_f \frac{L_{elem}}{D_{h,port}} \frac{G_{ref}^2}{2\rho_{ref}} \tag{23}$$

$$\frac{\partial p}{\partial z}_f = 8\left(\left(\frac{8}{Re_D}\right)^{12} + \left(\frac{1}{A+B}\right)^{1.5}\right)^{\frac{1}{12}} \tag{24}$$

$$A = (-2.456\ln^{0.9}\left(\frac{7}{Re_D}\right) + 0.27\frac{Ra_{tube}}{D_{h,port}})^{16} \tag{25}$$

$$B = \left(\frac{37530}{Re_D}\right)^{16} \tag{26}$$

in equation (23), L_{elem} is the tube length of each element, and G_{ref} is the mass flux of refrigerant in each tube.

Air side pressure drop is calculated by a equation set provided by Chang and Wang [?]:

$$f = f_1 f_2 f_3 \tag{27}$$

When $Re_{Lp} < 150$:

$$f_1 = 14.39Re_{Lp}^{-0.805\frac{P_{fin}}{D_{fin}}}\ln^{3.04}(1 + \frac{P_{fin}}{P_{louver}}) \tag{28}$$

$$f_2 = \ln^{-1.435}\left(\left(\frac{t_{fin}}{P_{fin}}\right)^{0.48} + 0.9\right)\left(\frac{D_{h,port}}{P_{louver}}\right)^{-3.01}\ln^{-3.01}(0.5Re_{Lp}) \tag{29}$$

$$f_3 = \left(\frac{P_{fin}}{L_{louver}}\right)^{-0.308}\left(\frac{D_{fin}}{L_{louver}}\right)^{-0.308}\exp(-0.1167\frac{P_{tube}}{h_{fin}})\theta_{louver}^{0.35} \tag{30}$$

When $150 < Re_{Lp} < 5000$:

$$f_1 = 4.97Re_{Lp}^{0.6049-1.064/\theta^{0.2}}(\ln((t_{fin}/P_{fin})^{0.5} + 0.9))^{-0.527} \tag{31}$$

$$f_2 = ((D_{h,port}/P_{louver})\ln(0.3Re_{Lp}))^{-2.966}(P_{fin}/L_{louver})^{-0.7931(P_{tube}/h_{fin})} \tag{32}$$

$$f_3 = (P_{tube}/t_{tube})^{-0.0446}(\ln(1.2 + (P_{louver}/P_{fin})^{1.4}))^{-3.553}\theta_{louver}^{-0.477} \tag{33}$$

The frictional factor f can also be expressed as:

$$f = \frac{A_c\rho_m}{A\rho_1}\left[\frac{2\rho_1 DP_{air}}{G_c^2} - (K_c + 1 - \sigma^2) - 2\left(\frac{\rho_1}{\rho_2} - 1\right) + (1 - \sigma^2 - K_e)\frac{\rho_1}{\rho_2}\right] \tag{34}$$

where G_c is the air mass flux after contraction; A_c is the free flow area, A is total surface area; ρ_1 and ρ_2 represents inlet and outlet air density respectively and ρ_m is the average density of inlet and outlet air; K_c and K_e are entrance and exit loss coefficients (the abrupt contraction and expansion coefficients) which are evaluated from Kays and London [6] at $Re_{Dh} = \infty$. With equation (33) and (34), we can calculate air side pressure drop. In this part, since the

outlet density cannot be determined with only tempearture, iteration is required.
By calculating one tube's thermal and hydraulic performance, the total energy transfer rate of the radiator is:

$$Q_{tot} = sum(Q_{elem})N_{tube,pass}N_{pass} \tag{35}$$

the outlet air temperature and pressure are approximated as the average of all the air outlet:

$$T_{ao} = ave(T_{ao,elem}) \tag{36}$$

$$P_{ao} = ave(P_{ao,elem}) \tag{37}$$

the water-EG outlet temperature and pressure are taken as the calculated tube outlet temperature and pressure.

RESULTS AND DISCUSSION

The simulation is conducted with the number of segments ranging from 1 to 50. The detailed thermal and hydraulic performance through one tube are shown in Figure 4 and 5, which are computed with number of segments 40. The overall performance of the radiator - the heat transfer rate, discharge temperature, and pressure drop are included in Table 5. The cooling capacity of the radiator is around 26.33kW, with coolant outlet temperature at 64.18°C.
According to Figure 5, as coolant flows through the tube, the coolant pressure drop keeps increasing, since lower temperature of coolant leads to higher viscosity; because the temperature difference between the coolant and air decreases as coolant flows, the heat transfer rate decreases. For the air side, the friction factor f is determined by the geometry of the tube and fin, which is constant; however, since the heat transfer rate decreases, the density ratio of inlet and outlet air becomes smaller, i.e. $\frac{\rho_1}{\rho_2}$ in equation (34), and the pressure drop of air side decreases.
As the number of segment increases from 1 to 50, the thermal and hydraulic performance converged as shown in Figure 6. Theoretically, larger mesh size can have higher accuracy; however, when segment number is higher than around 25, increasing mesh size does not have a big impact on the result but increasing computation time. Thus, it is not always a good idea to increase the segment number, and a proper mesh size is critical for a simulation.
Figure 7 shows the impact of the air mass flow rate from 4000kg/h to 6000kg/h at $N_{segment}$ = 40 to the simulation results. As the air mass flow rate increases, the thermal performance of the radiator is improved. The outlet coolant temperature decreases around 2% and the cool-

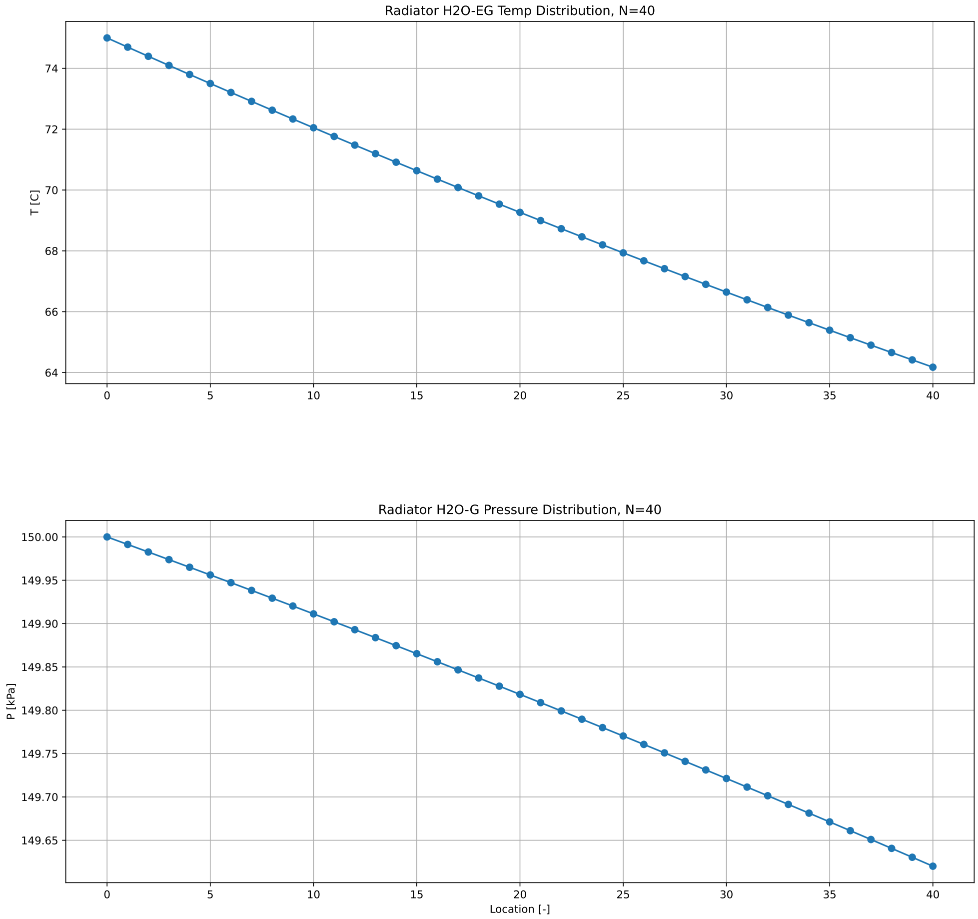

Figure 4: Detailed thermal performance, coolant side, $N_{segment} = 40$

ing capacity of the radiator increases around 16.7%. However, the pressure drop of coolant side and air side increases. And the Figure shows a slightly trend of converging, which means keep increasing air mass flow rate is not always a good idea to improve cooling performance of the radiator. Consider that the automobile can drive at a high speed which will help with thermal dissipation; but if the automobile is driving at a low speed, increase cooling capacity by increasing fan speed is not wise because higher fan speed can cause power consumption increase dramatically.

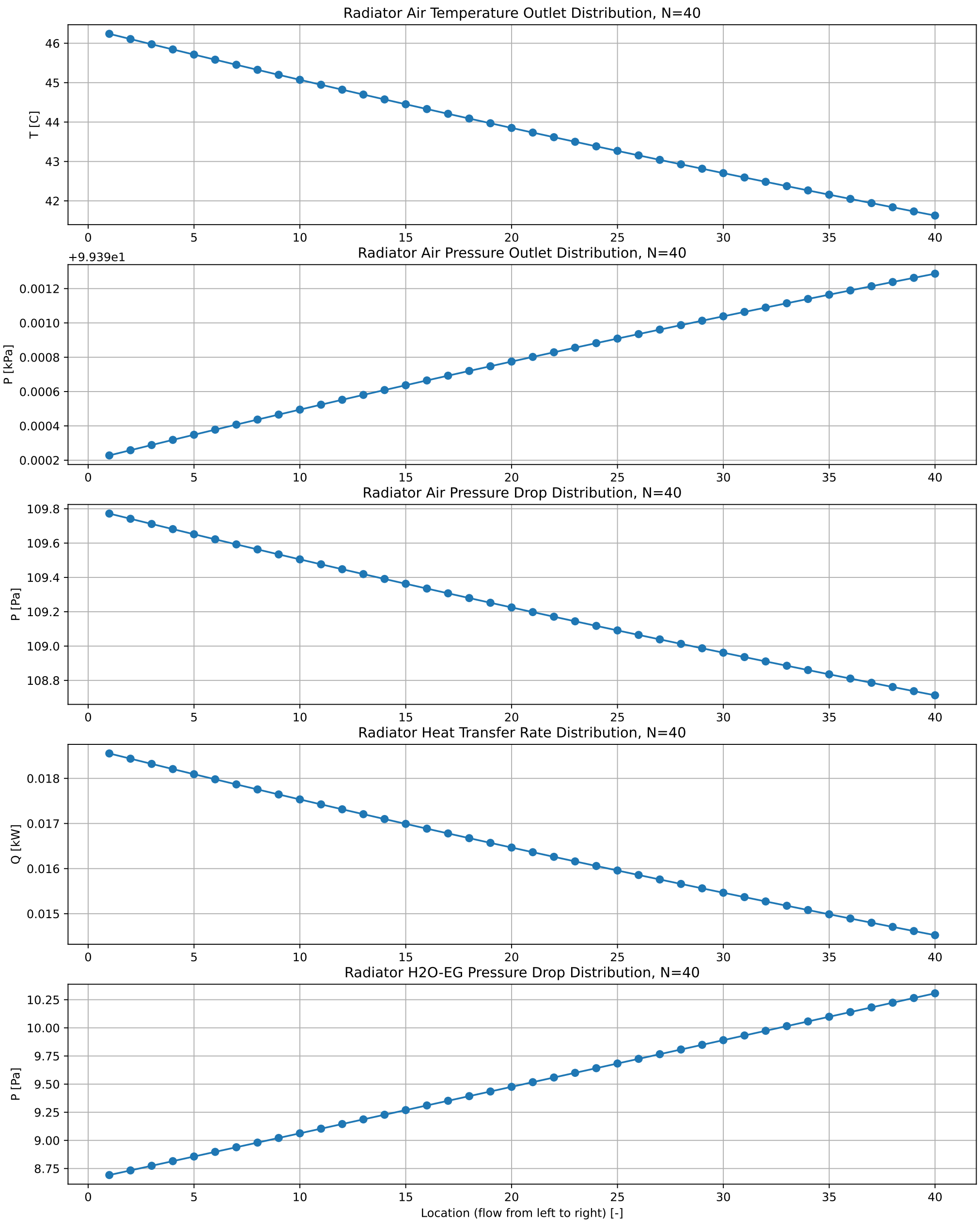

Figure 5: Detailed thermal performance, coolant side, air side, $N_{segment} = 40$

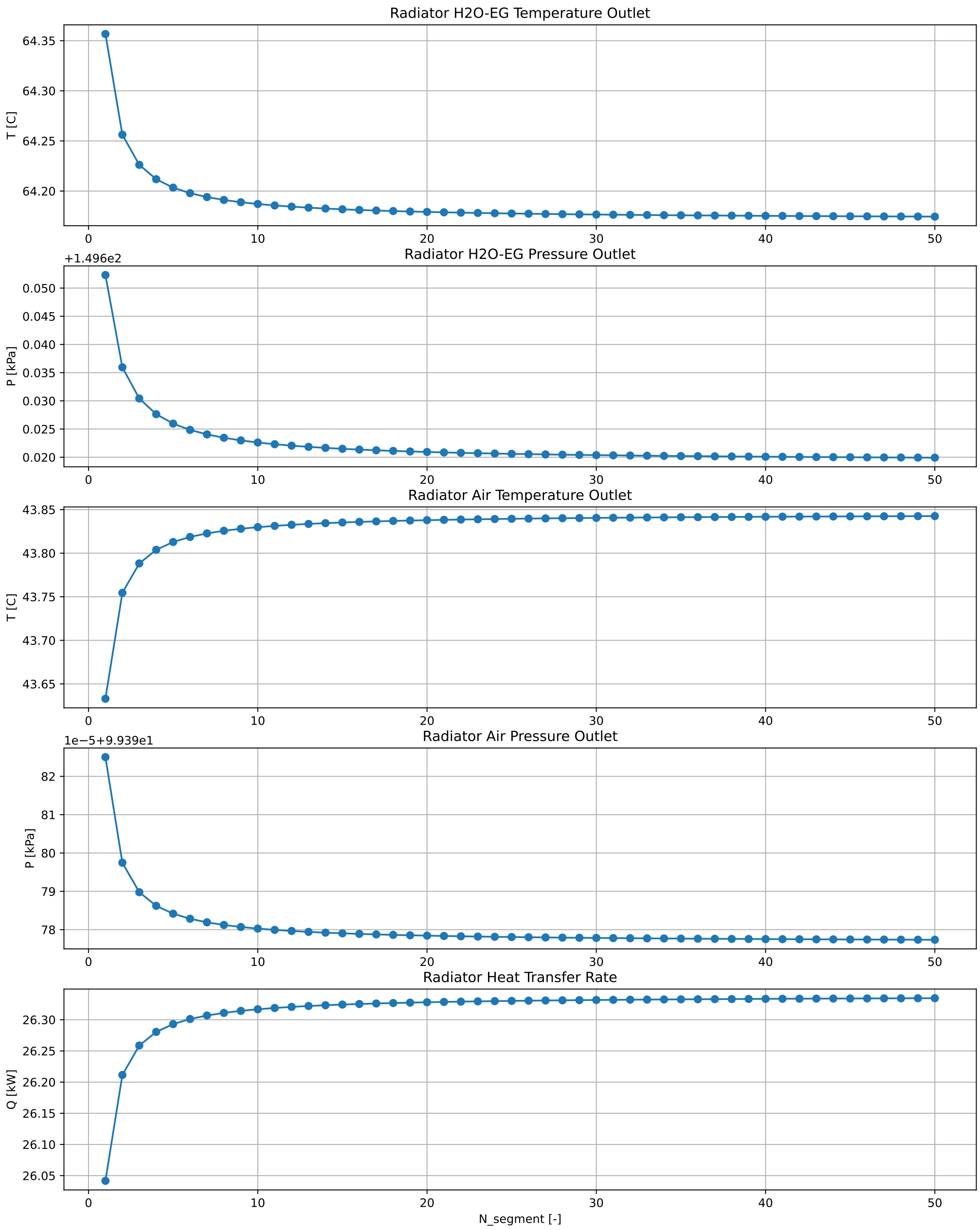

Figure 6: Segment number impact to simulation of radiator

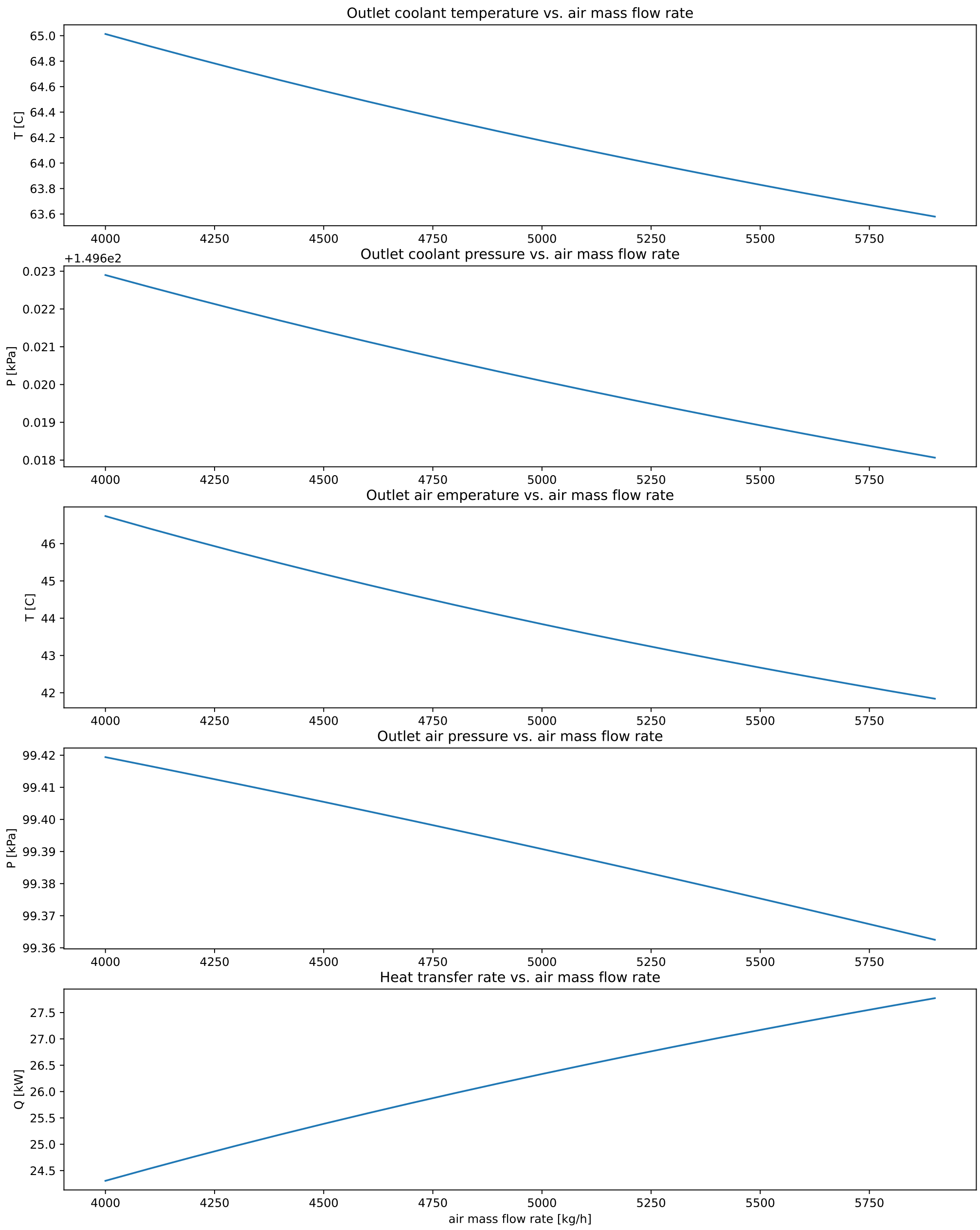

Figure 7: Air mass flow rate impact to simulation of radiator

Parameter	Value
T_{ro}: refrigerant outlet temperature, [C]	64.18
P_{ro}: refrigerant outlet pressure , [kPa]	149.62
T_{ao}: air outlet temperature, [C]	43.84
P_{ao}: air outlet pressure, [kPa]	99.39
Q_{tot}: total heat transfer rate, [kW]	26.33

Table 5: Overall performance of radiator, $N_{segment} = 40$

CONCLUSIONS

This project studied about simulation for radiator thermal and hydraulic performance. The impact of air mass flow rate and mesh size is discussed. There should be a optimized mesh size for each simulation with consideration of accuracy and computation time. Increasing air mass flow rate can increase the cooling capacity of radiator, but it has limitations that the improvement is minor and it has a trend to converge.

To improve the thermal performance of radiator, the geometry of radiator should be paid with more attention. Besides, this project has no validation of experimental result. The accuracy of the model needs to be further investigated. The assumption made for the coolant mass flow distribution should be reconsidered, since in real condition, the coolant enter the radiator from the top of the header (as shown in Figure 3), the uniform mass distribution is not valid. The air properties used in this project is for ideal gas; although there is no condensation or frosting in current simulation, for vehicle in cold weather, considering the relative humidity is important.

References

[1] Chang, Y-JY-J., et al. "A generalized friction correlation for louver fin geometry." International journal of heat and mass transfer 43.12 (2000): 2237-2243.

[2] Chang, Yu-Juei, and Chi-Chuan Wang. "Air side performance of brazed aluminum heat exchangers." Journal of Enhanced Heat Transfer 3.1 (1996).

[3] Gnielinski, Volker. "New equations for heat and mass transfer in the turbulent flow in pipes and channels." NASA STI/recon technical report A 41.1 (1975): 8-16.

[4] Churchill, Stuart W. "Friction-factor equation spans all fluid-flow regimes." (1977).

[5] Chang, Y-JY-J., et al. "A generalized friction correlation for louver fin geometry." International journal of heat and mass transfer 43.12 (2000): 2237-2243.

[6] Kays, William Morrow, and Alexander Louis London. "Compact heat exchangers." (1984).